Evaluation of Incremental Reactivity and Its Uncertainty in the South Coast Air Basin

Philip T. Martien and Robert A. Harley

Dept. of Civil and Environmental Engineering, University of California, Berkeley, CA 94720-1710

Jana B. Milford

Dept. of Mechanical Engineering, University of Colorado, Boulder, CO 80309-0427

Armistead G. Russell

School of Civil and Environmental Engineering, Georgia Institute of Technology, Atlanta, GA 30332-0512

Abstract

The incremental reactivity (IR) and relative incremental reactivity (RIR) of carbon monoxide and 30 individual volatile organic compounds (VOC) were estimated for the South Coast Air Basin using two photochemical air quality models: a 3-D, grid-based model and a vertically-resolved trajectory model. Both models include an extended version of the SAPRC99 chemical mechanism. For the 3-D modeling, the decoupled direct method (DDM-3D) was used to assess reactivities. The trajectory model was applied to estimate uncertainties in reactivities due to uncertainties in chemical rate parameters, deposition parameters, and emission rates using Monte Carlo analysis with Latin hypercube sampling. For most VOC, RIRs were found to be consistent in rankings with those produced by Carter using a box model. However, 3-D simulations show that coastal regions, upwind of most of the emissions, have comparatively low

IR but higher RIR than predicted by box models for C_4-C_5 alkenes and carbonyls that initiate the production of HO_x radicals. Biogenic VOC emissions were found to have a lower RIR than predicted by box model estimates, because emissions of these VOC were mostly downwind of the areas of primary ozone production. Uncertainties in RIR of individual VOC were found to be dominated by uncertainties in the rate parameters of their primary oxidation reactions. The coefficient of variation (COV) of most RIR values ranged from 20% to 30%; whereas, the COV of absolute incremental reactivity ranged from about 30% to 40%. In general, uncertainty and variability both decreased when relative rather than absolute reactivity metrics were used.

1. Introduction

Volatile organic compounds (VOC) and oxides of nitrogen (NO_x) are the main reactants in the photochemical reactions that produce ozone in the troposphere. Individual VOC are known to differ significantly in both the rates and in the products of their oxidation reactions [1]. These differences can have a significant effect on ozone formation [2]. Consequently, in developing strategies to reduce the formation of ozone, ignoring the reactivity of emissions may lead to ineffective and inefficient controls, while consideration of reactivity focuses control efforts on those VOC with the greatest impacts on ozone.

Carter [2] used a box model with a detailed chemical mechanism to quantify the ozone formed from 180 different VOC in 39 cities across the United States. Eighteen different reactivity scales were developed from those model calculations. The incremental reactivity (IR) of a VOC is operationally defined as the change in peak ozone produced by a small increase in emissions of that VOC. IR scales can differ with different assumptions about the levels of NO_x and the method used to measure the ozone impact; some measures examined the effects on

peak ozone and others examined the integrated impacts over a period of time. The Maximum Incremental Reactivity (MIR) scale is determined by adjusting the input ratio of VOC to NO_x to maximize the incremental reactivity of a base VOC mixture. MIR of an individual VOC species is most commonly defined as

$$MIR_i = \frac{\partial [O_3]_p}{\partial E_i} \text{ at VOC/NO}_x \text{ for maximum IR of base mix} \quad (1)$$

where $[O_3]_p$ represents the peak ozone concentration and E_i represents emissions of the VOC species. The MIR scale has been used to compare the reactivity of exhaust emissions from alternatively fueled vehicles to the reactivity of exhaust emissions from a vehicle using conventional gasoline [3].

MIR conditions occur at relatively low VOC/NO_x ratios (4-6 ppmC : 1 ppm NO_x), as might be found in many urban areas. At lower NO_x levels, the absolute incremental reactivity of individual VOC is expected to be less than under MIR conditions. To investigate this effect, Carter [2] developed several alternative scales, including maximum ozone incremental reactivity (MOIR). MOIR is evaluated at higher VOC/NO_x ratios of about 8:1, conditions that lead to maximum ozone (in contrast, MIR conditions correspond to maximum sensitivity of ozone to VOC). Nevertheless, the ranking of VOC species based on MOIR is similar to that derived using the MIR scale.

Since Carter developed reactivity scales using a 0-D box model, an issue of concern is how applicable VOC rankings based on such scales are to a real, three-dimensional air basin. For example, the spatial distribution of the emissions of a VOC could influence its reactivity. Furthermore, the MIR scale was developed based on 10-hour simulations, whereas some organic

compounds may remain in an urban airshed for 2 to 3 days. Previous investigators [4, 5, 3, 6] applied 3-D air quality models to California's South Coast Air Basin (SoCAB) and compared their results to box-model results. In general, these studies found that if VOC reactivities are compared on a relative basis, the 0-D and 3-D results are similar for most of the compounds investigated. However, for some species, notable differences in reactivity were reported.

Another concern is that quantification of VOC reactivities is limited by uncertainties in our knowledge of atmospheric chemistry. Measurement errors in laboratory kinetic and product studies contribute to uncertainty in the chemical mechanisms used to calculate incremental reactivities. Moreover, the reactions of many of the organic compounds emitted into urban atmospheres have never been studied in controlled experiments. Their representation in chemical mechanisms is based on analogy to compounds of similar structure, creating added uncertainty. At issue is whether the uncertainties in the chemistry significantly affect the calculation of the reactivities for organic compounds. Previous studies using a box model [7, 8] and an airshed model [3, 9] have explored to what degree uncertainties in chemical reaction parameters affect calculated reactivities. These studies suggested that control strategies based on relative reactivity were robust with respect to uncertainty in the chemistry.

In this study, recently developed techniques are applied to examine incremental reactivity, its spatial variability, and its sources of uncertainty in a real air basin. As in the study by Kahn et al. [6], this study uses the decoupled direct method to estimate reactivities. We use an updated chemical mechanism and look specifically at the effects of spatial distribution of emissions (including biogenic emissions) and compare the reactivity rankings of 30 VOC species and CO at individual sites. The objectives of this study are to (1) apply a 3-D model to assess the reactivity of individual VOC with respect to ozone formation; (2) compare relative

incremental reactivities computed using the 3-D model with Carter's reactivity scales computed using a box model; and (3) conduct a formal sensitivity and uncertainty analysis of incremental reactivity for the same time and location using a photochemical trajectory model to identify the most important factors contributing to uncertainty in reactivity assessments.

2. Methodology

a. Chemical Mechanism

The chemical mechanism used in this study is an extended version of the SAPRC99 mechanism [10]. SAPRC99 incorporates rate coefficients, absorption cross sections, quantum yields and mechanistic parameters that were updated based on reviews conducted over the past decade (see Carter [10] for details). Compared to previous versions of the mechanism [11, 12], the most significant change made to the inorganic chemistry was reducing the OH + NO_2 rate constant by approximately 30%, as recommended by DeMore et al. [13].

In this research, 31 chemical species were identified for detailed incremental reactivity calculations (Table 1). These species represent most of the important classes of VOC, including compounds of anthropogenic and biogenic origin. The base SAPRC99 mechanism was extended to represent each of these species explicitly, using reactions provided by Carter [10].

The extended mechanism contains 104 species and 246 reactions (see Martien et al. [14] for a complete listing of the extended mechanism). Of the 104 species, eight are lumped primary organic species: ALK1, ALK2, and ALK3 representing alkanes; ARO1 and ARO2 representing aromatics; OLE1 and OLE2 representing alkenes; and TRP1 representing terpenes. We use fixed oxidation product yields for all lumped organic species.

b. The Decoupled Direct Method

Most previous studies of incremental reactivity used a finite-difference approximation method (also known as the "brute force" method) to estimate IR from calculated O_3 concentrations at known emission levels:

$$\frac{\partial [O_3]_p}{\partial E_i} \approx \frac{[O_3]_p(E_i + \Delta E_i) - [O_3]_p(E_i)}{\Delta E_i} \tag{2}$$

To improve efficiency for 3-D assessments of IR in this study, we applied the decoupled direct method or DDM [15], as demonstrated by Yang et al. [16]. In DDM-3D, a set of sensitivity equations is derived from the atmospheric diffusion equation:

$$\frac{\partial c_i}{\partial t} + \nabla \cdot (\mathbf{u} c_i) = \nabla \cdot (K \nabla c_i) + R_i(c_1, \cdots, c_N) + Q_i(\mathbf{x}, t) \tag{3}$$

In eq 3, c_i is the concentration of species i, $\mathbf{u}$ is the wind velocity vector, K is the diffusivity tensor, R_i is the net rate of formation of compound i due to chemical reactions, Q_i is the source term for compound i due to emissions, and N is the number of species being tracked in the model. This coupled system of equations is solved numerically subject to initial and boundary conditions [17].

To obtain the semi-normalized sensitivity, $s^*_{i,j} = E_j \partial c_i / \partial E_j$, of the concentration of species i to the emissions of species j, the governing equations and boundary conditions are differentiated with respect to a multiplicative emissions scaling factor, ϵ_j:

$$\frac{\partial s^*_{i,j}}{\partial t} + \nabla \cdot (\mathbf{u} s^*_{i,j}) = \nabla \cdot (K \nabla s^*_{i,j}) + J_{i,k} s^*_{k,j} + \frac{\partial R_i}{\partial \epsilon_j} + \frac{\partial Q_i(\mathbf{x}, t)}{\partial \epsilon_j} \tag{4}$$

Factor ϵ_j has a nominal value of 1 and is applied uniformly throughout the spatial domain and time period of the simulation. For the present study c_i represents the concentration of ozone and ϵ_j are scaling factors applied to the emissions of individual VOC. Sensitivity coefficients are calculated during the same model run used to calculate species concentrations, by alternating the solution of eqs 3 and 4.

c. Incremental Reactivity Scales

Absolute incremental reactivity (AIR) was derived from $s^*_{i,j}$ values predicted at the time of peak observed ozone at receptor locations of interest:

$$AIR_j = \frac{s^*_{i,j}}{MW_j \; E_j} \tag{5}$$

where $s^*_{i,j}$ is the semi-normalized sensitivity of ozone (ppm O_3) with respect to a dimensionless multiplier ϵ_j applied to emissions of species j at all locations and times. MW_j is the molecular weight and E_j is the molar emissions rate of species j throughout the modeling domain.

Differences in the chemical environment of individual receptor locations, including differences in the amount and timing of upwind VOC and NO_x emissions, are expected to affect AIR values calculated from eq 5. Previous studies have suggested that normalizing reactivities to the reactivity of a base mixture of compounds should decrease their variability [5]. In this study, relative incremental reactivities (RIRs) are calculated as

$$RIR_j = \frac{AIR_j}{\sum_k \; w_k \; AIR_k} \tag{6}$$

where AIR_k is the absolute reactivity of the k^{th} compound and w_k is its mass fraction in

the mixture. The compounds included in the mixture and their assumed mass fractions were 2% formaldehyde, 14% MEK, 37% n-butane, 26% 2,2,4-trimethylpentane, 2% propene, 17% ethanol, and 2% m-xylene. The mass fractions were set such that compounds would contribute equally to the reactivity of the mixture based on trajectory model calculations for a trajectory ending at Claremont. Note that this weighting is specific to this study, so that the RIR values are only comparable within the study.

d. Application to the South Coast Air Basin

The model was applied to a historical air pollution episode, 23-25 June 1987. An extensive meteorological and air-quality-monitoring network that exists in Southern California was used to specify meteorological inputs and initial conditions for the air quality models. Supplemental upper air soundings were conducted during the Southern California Air Quality Study (SCAQS) for the 24-25 June 1987 intensive monitoring period. These soundings were performed every 4 hours at a network of 8 sites located along the coast and inland. Mixing depths were determined as the height to the base of the inversion layer in plots of potential temperature versus altitude. Mixing depths, temperatures, surface winds, and winds aloft were interpolated using objective analysis procedures [18, 19] to derive spatially and temporally complete meteorological fields. Similar interpolation procedures were applied to observed concentrations of CO, NO, NO_2, O_3, and NMHC to derive initial conditions for these pollutants. By starting model simulations at 1600 PST on 23 June 1987, observed pollutant concentrations at the surface could be used to estimate pollutant levels throughout the mixed layer. These input data were developed and used in a previous photochemical modeling study of the same episode [20]. Inflow boundary conditions were based on a review of measurements of pollutant concentrations at San Nicolas

Island and in aircraft studies conducted offshore of southern California [21].

Figure 1 shows the study domain and the boundary of the computational region. It also shows 8 sites at which IR was evaluated. The coastal sites at Hawthorne and Long Beach are characterized by coastal breezes and relatively clean air. Further inland, the Central Los Angeles and Anaheim sites are located in a region of high emissions and increased levels of air pollution. The inland sites Burbank, Azusa, Claremont, and Rubidoux are downwind of the core urban areas in the computational domain and downwind of most of the emissions. The inland sites experienced the highest levels of ozone during the study period.

Emission inventory estimates used in this research were provided by the California Air Resources Board [22]. Estimates of mobile, area, and point source emissions are for summer 1987 typical weekday conditions. Emissions from motor vehicles were revised using a fuel-based inventory approach [23]. CO emissions were based on fuel sales and an on-road infrared remote sensing study of vehicle CO emissions conducted in southern California shortly after the 1987 SCAQS field experiment [23]. Ratios of NMOC/CO and NO_x/CO in vehicle emissions were calculated via regression analysis of ambient pollutant concentrations measured during SCAQS for morning commuter peak periods. The product of these ratios and the CO emissions yielded VOC and NO_x emissions estimates.

The spatial distribution of daily total emissions of selected VOC are shown in Figure 2. Propene emissions, the primary source of which is automobile exhaust, are heavily concentrated in the central urbanized portion of the modeling domain. Likewise, isopropanol emissions due mostly to evaporating solvents, are also concentrated in the central region. Emissions of isoprene, which are almost all biogenic, are distributed mostly to the north and east and downwind of the urbanized region.

All 3-D model simulations started at 1600 PST on 23 June 1987 and continued until 2400 PST on 25 June. Calculations of VOC reactivity were made for 25 June in order to minimize the influence of uncertainties in initial conditions on the results.

e. Uncertainty Analysis

Monte Carlo analysis with Latin hypercube sampling [24] was used to estimate uncertainties in base case ozone concentrations and in incremental reactivity estimates. The uncertainty analysis was conducted using a 1-D trajectory version of the air quality model [25]. Multi-day back-trajectories were computed so that air parcels arrived at each of the receptor air monitoring sites of interest at the time of maximum observed ozone. A total of 33 uncertain input parameters were treated as random variables, as listed in Table 2. These parameters include rate coefficients, product yields, emissions rates and deposition parameters determined previously to be influential for box model reactivity calculations [26], or for the response of ozone concentrations to VOC emissions reductions [25]. Unless indicated otherwise in Table 2, all of the uncertainties were incorporated in the model as multiplicative factors, drawn from independent lognormal distributions with a mean of 1.0. The derivations or sources for uncertainty estimates are given in Bergin et al. [25] unless otherwise noted. Multivariate linear regression analysis was applied to the Monte Carlo results to identify the influence of input variables on incremental reactivity estimates.

Motor vehicle emissions and associated uncertainty estimates were defined using results of previous research [23, 25]. The EMCO variable listed in Table 2 represents the uncertainty common to motor vehicle emissions of all pollutants (i.e. CO, NMOC, and NO_x), and was estimated from site-to-site variability in on-road remote sensing measurements for CO emissions.

This uncertainty applies not only to CO, but also to the other pollutants, because NMOC and NO_x emissions were estimated as the product of CO emissions and ambient pollutant ratios, as described in the previous section. Additional, independent uncertainties in NMOC and NO_x emissions from motor vehicles are represented by the parameters EMHC and EMNX. These additional uncertainties, which are relatively small, arise from the uncertainties in the regression analysis of ambient concentrations of NMOC and NO_x versus CO.

3. Results and Discussion

a. Performance Evaluation

Model performance statistics for ozone indicate that the 3-D model simulated observed surface-level ozone in this episode with a low bias and a moderate amount of error. Performance statistics on 24 and 25 June were similar: normalized bias was +7% and the normalized gross error was 42% on both days for surface-level ozone above 60 ppb. Time series plots (Figure 3) show consistency between observed and simulated ozone at the 8 sites where AIR and RIR were calculated. At coastal sites Hawthorne and Long Beach, observed and predicted maximum ozone was about 70 ppb on both 24 and 25 June. Nighttime simulated ozone was predicted to be near zero, whereas the observed ozone concentration was about 40 ppb at this time. At the central and inland sites, the magnitudes of the daily ozone peaks were usually within about 30 ppb of the observations, and the times of the predicted peaks were within about an hour of the observed peak. Observed nighttime ozone values at the central and inland sites were near zero; nighttime model predictions matched these observations.

b. Incremental Reactivity

Absolute reactivity was found to vary significantly within the domain. Figure 4 shows AIR values at the time of maximum observed ozone at two locations. Figure 4 indicates that AIR at the coastal Hawthorne site is nearly an order of magnitude smaller than at the inland Claremont site. Hawthorne and other coastal sites are upwind of most emissions, so ozone at these sites is only slightly reduced by VOC emission reductions. In contrast, at Claremont and other inland sites, VOC reductions significantly reduce ozone.

Simulated AIR is low at the coastal sites, increases near the central sites, and then decreases again at the furthest inland (downwind) sites. The highest AIR values occur near Azusa. The spatial distribution of AIR suggests an analogy between the variation in VOC/NO_x ratio at different locations and the adjustments made by Carter [2] to VOC/NO_x ratios to create either MIR or MOIR conditions. By this analogy, maximum ozone conditions on both 24 and 25 June are achieved near Claremont; while maximum incremental reactivity conditions are achieved near Azusa on both days. However, this analogy is not perfect because the VOC/NO_x ratio is not the only quantity varying: the reactivity of the VOC mix and the concentration of precursors vary at different locations as well.

Measures of relative reactivity (RIR from eq 6) at 8 sites are presented in Figure 5 for 25 of the 30 VOC. Relative MIR (R_MIR) values are shown for comparison, based on MIR values from Carter [27] and again using eq 6 to compute relative values. In these figures, sites are ordered from coastal to inland. Note that the scaling of the vertical axis varies.

The alkanes were not found to be particularly reactive. Most of the alkanes have RIR values calculated from 3-D modeling that are consistent with Carter's R_MIR. Notable exceptions are n-butane and n-pentane at Long Beach. This site is characterized by high concentrations of these compounds due to nearby refinery emissions; thus, ozone at this site is relatively more

affected by changes in emissions of these n-alkanes.

Alkenes are generally more reactive than the alkanes, as shown in Figure 5. There are notable differences in the comparison to the R_MIR values. At the coastal and central sites for many of the alkenes, the estimated values of RIR from DDM-3D tend to be larger than the corresponding R_MIR values. At these locations, concentrations of radical species tend to be relatively low and alkenes, whose direct reactions with ozone initiate the production of HO_x radicals, therefore have a larger effect on ozone than they would at locations with a rich supply of radicals.

Important exceptions to the tendency for alkene RIR to be greater than R_MIR are the biogenic species isoprene and α-pinene. R_MIR values for both isoprene and α-pinene are higher than the corresponding DDM-3D estimates at all 8 sites. This difference is due to the spatial distribution of the biogenic emissions. As noted in the discussion of Figure 2 above, the distribution of biogenic emissions places most of the isoprene and α-pinene downwind of these sites. Therefore, the effect of these species on ozone is reduced relative to what would be predicted if the spatial distribution of emissions matched that of anthropogenic VOC.

Across the 8 sites, the estimated RIR values for aromatic species shown in Figure 5 are close to, but generally lower than R_MIR values. There is a trend of increasing RIR from Hawthorne to Anaheim and a trend of decreasing RIR from Anaheim to Rubidoux. Apparently conditions at the Anaheim site are near the conditions for maximum incremental reactivity of aromatics. RIR values at Anaheim agree most closely with R_MIR values.

The values of RIR for most of the carbonyls shown in Figure 5 are consistent for a given species across sites. For some species, RIR and R_MIR values also agree. There are several notable exceptions where significant variations are evident. The reactivity of formaldehyde

varies widely from site to site and generally decreases from coastal to inland sites. Formaldehyde photolysis can initiate the formation of radicals ($HCHO + h\nu \rightarrow 2HO_2^{\bullet} + CO$). At sites where low radical concentrations limit production of ozone, formaldehyde has particularly high RIR values. Interestingly, benzaldehyde RIR values at all sites and the R_MIR value are negative. This is because there is a NO_x sink in the reaction mechanism for benzaldehyde, which results in an overall reduction in ozone formation [28]. At the Hawthorne site only, acetaldehyde has a negative RIR value. Propionaldehyde and benzaldehyde also show decreases in RIR at Hawthorne relative to other sites. These aldehydes are precursors to peroxyacetyl nitrate (PAN) and its analogs; formation of PAN competes with NO_2 photolysis that would otherwise form ozone. Other species showed no exceptional trends and are not shown in Figure 5, but are discussed in the context of Figure 6 below.

Figure 6 plots the 8-site average RIR for each species ranked in order of the R_MIR values from the box model. Figure 6 plots the 8-site average RIR ranked in MIR order for each species. For comparison, the corresponding R_MIR values (mean of 39 scenarios) are also plotted. Error bars show $\pm$ 1 standard deviation, indicating variability across locations for each case. For most species the sort order for DDM-3D RIR does not shift by many positions relative to R_MIR from the box model. An exception to this is formaldehyde, which, as noted above, is an important chain initiator for radical species. For coastal and central locations, formaldehyde moves up in the rank order. While the rankings of anthropogenic alkenes such as 2-methyl-2-butene are high in all cases, the reactivity of these alkenes is much higher, on a relative basis, at coastal sites compared to inland sites. RIR for these species has a large site-to-site variation. The biogenic species isoprene and α-pinene stand out in Figure 6; these compounds would move down in sort order if ranked by DDM-3D RIR values. The reason for this, as noted above, is

that the spatial distribution of the biogenic emissions is such that most of the emissions occur downwind of the sites examined here.

Other species (defined in Table 1) all have mean RIR values of 0.5 or less. While there is fair agreement with R_MIR values, the R_MIR values are larger than the 8-site mean of the RIR values. There is a tendency for increasing RIR values of these other species with distance from the coast. This trend is probably due to the increase in radical availability at inland sites and the fact that alkenes and formaldehyde are relatively high at the coastal and central sites.

The RIR at inland sites follow more closely the rankings based on MIR. At the inland sites, formaldehyde falls more nearly into the MIR ranking. However, note that the RIR values of the biogenic species are still greatly reduced and would drop in rank order even at the inland sites.

c. Uncertainty and Variability

Figure 7 shows absolute incremental reactivities (AIR) for eight compounds and the base mixture, calculated from the ozone concentrations at the endpoints of four trajectories. Average AIR values from the Monte Carlo simulations are shown, with associated error bars indicating standard deviations from the Monte Carlo analysis. For HCHO, n-butane, propene, m-xylene and the base mixture, incremental reactivities are lowest for the Rubidoux trajectory, while those for ethanol and MEK are lowest for the Anaheim trajectory. The coefficients of variation (COV = standard deviation divided by the mean) for the eight compounds and base mixture range from 0.16 for m-xylene at Anaheim to 0.63 for HCHO at Rubidoux, with most of the COV values falling in the range of 0.3 to 0.4. Uncertainty in the AIRs is generally highest at Rubidoux.

Relative incremental reactivities (RIR) for eight compounds are also shown in Figure 7. Accounting for uncertainties in the inputs for a given trajectory, COVs for the RIRs range from 0.08 for propene at Anaheim and Azusa to 0.49 for CO at Rubidoux. COVs for most of the RIRs range from 0.2 to 0.35. With few exceptions, uncertainties in RIRs are lower than those in AIRs. In general, normalizing reactivities also reduces variability across locations. Comparing Figures 7a and 7b, RIRs for all compounds except CO and ethanol are less variable across trajectories than AIRs. For the eight compounds shown, the coefficients of variation across trajectories in the average AIRs range from 8% for CO and 2,2,4-trimethylpentane to 37% for MEK and 39% for HCHO (Figure 7a). The coefficients of variation in the RIRs across trajectories range from 7% for propene to 35% for both ethanol and MEK.

Table 3 shows the average and COV of AIR for the base mixture calculated at the end-points of each trajectory. It also shows regression results, indicating which model parameters contribute the most to uncertainty in AIR values. The eight uncertain input parameters with the greatest influence on uncertainty in the AIR estimates are shown for the base mixture. A total of 16 parameters are included in the top eight for one or more of the trajectories. Six of them, the rate parameters for $NO_2 + h\nu$, $HCHO + h\nu$, $O_3 + h\nu$, $OH + NO_2$ and PAN decomposition, and the emissions rates for non-mobile NO_x emissions, appear in the top eight for three locations.

The sign of the standardized regression coefficients indicates the sign of the response of the mixture incremental reactivity to an increase in the value of each parameter. Parameters with positive regression coefficients in Table 3 are shown in bold text; those with negative coefficients are shown in normal text. These signs differ across the trajectories for parameters that control the amount of NO_x or radicals in the air parcel. For Claremont and Rubidoux, the incremental

reactivity of the mixture increases with increased NO_x emissions or a reduced NO_2 deposition rate. For Azusa, the sensitivity of the mixture AIR to increased NO_x emissions or reduced NO_2 deposition is negative. The mixture AIR for Anaheim is relatively insensitive to these parameters. The incremental reactivity of the base mixture for Rubidoux displays negative sensitivity to parameters that would increase the supply of radicals (e.g., $O_3 + h\nu$, $HCHO + h\nu$) while the opposite is true for Anaheim and Azusa.

Regression results for RIRs of individual compounds are shown in Table 4. Representative results from this table are discussed below, beginning with those for the less reactive compounds such as n-butane.

For all four trajectory endpoints, the RIR of n-butane is sensitive to the rate constant for its reaction with OH, and to parameters that control the availability of OH radicals. Regression results for CO and 2,2,4-trimethylpentane are similar, showing high positive sensitivity to their OH reaction rates and to reaction rates for $O_3 + h\nu$ and $O^1D + H_2O$, and negative sensitivity to reaction rates for $OH + NO_2$, and $O^1D + M$. As shown in Table 4, regression results for the ethanol are different from those of other slowly reacting compounds, due to the influence of uncertainties in PAN chemistry. Results for ethanol are relatively consistent across trajectories. In contrast to those compounds that react only with OH, the primary oxidation pathway for MEK is its photolysis reaction. At all four locations, the RIR for MEK is most sensitive to the rate of this reaction. In contrast to the low-reactivity compounds that are oxidized by OH, the RIR for MEK is also strongly negatively influenced by parameters that increase the rate of OH production or reduce its consumption rate (e.g., $OH + NO_2$).

Among the more reactive species, the RIR for HCHO is generally sensitive to parameters that affect other sources and sinks of radicals such as $O_3 + h\nu$, and displays negative sensitivity

to parameters that increase the AIR of other components of the base mixture, including the rate constants for $NO_2 + h\nu$ and CCO-O2 + NO. Uncertainty in the HCHO photolysis rate is highly influential for the HCHO RIR value of the Anaheim and Azusa trajectories but not for the relatively NO_x-limited trajectories ending at Claremont and Rubidoux. The results shown in Table 4 for m-xylene are typical of those for other rapidly reacting compounds such as propene, which react primarily with OH. Parameters of the m-xylene reaction mechanism that directly affect its absolute reactivity, such as the rate constant for its reaction with OH and its dicarbonyl (DCB2) yield, are influential. Otherwise, the m-xylene RIR shows strong negative sensitivity to parameters that increase the reactivity of other compounds in the base mixture, including the rate constants for their primary oxidation reaction steps and rates of reactions that produce hydroxyl or peroxy radicals. Although the order changes, the set of parameters that are most influential for m-xylene is relatively consistent across trajectories.

RIRs for several compounds show relatively high sensitivity to uncertainty in emissions rates. The responses are mixed, with the sign of the RIR sensitivities determined by whether the AIR of the compound is more or less sensitive to the emissions parameter than the incremental reactivity of the base mixture. For example, at Claremont and Rubidoux, the AIR of the base mixture displays a positive sensitivity to the non-motor vehicle NO_x emissions (EONX) parameter, as do formaldehyde and CO. However, the absolute reactivity of CO and HCHO, respectively, are less and more sensitive to EONX than the AIR of the base mixture. Correspondingly, sensitivity coefficients for CO RIR values are negative and those for HCHO RIR values are positive.

Calculated incremental reactivities for organic compounds are subject to both variability due to environmental conditions, including the magnitude and timing of emissions, and uncertainty

due to model inputs and parameter values. The results of this study suggest that for this air pollution episode, variability in RIR estimates across locations within the South Coast Air Basin is comparable in magnitude to the uncertainty in RIR that is attributable to chemical and deposition parameters and emissions inputs. A distinction that is often made between variability and uncertainty is that the former is irreducible, for a given metric, whereas the latter may be reduced through research. This study supports previous studies [5, 29] that suggest that using relative rather than absolute reactivity metrics can reduce both variability and uncertainty.

4. Acknowledgments

We thank Dr. William Carter of UC Riverside for technical assistance and helpful discussions, Greg Noblet of UC Berkeley for assistance in developing input data files, and Stephanie Rivale of CU Boulder for help with the uncertainty calculations. This work was supported by the California Air Resources Board under contract 98-309. The statements and conclusions herein are those of the authors and not necessarily those of the California Air Resources Board.

References

[1] Atkinson, R. *Atmos. Environ.*, **2000**, *34*, 2063–2101.

[2] Carter, W. P. L. *J. Air Waste Manage. Assoc.*, **1994**, *44*, 881–899.

[3] Bergin, M. S.; Russell, A. G.; Milford, J. B. *Environ. Sci. Technol.*, **1995**, *29*, 3029–3037.

[4] McNair, L. A.; Russell, A. G.; Odman, M. T. *J. Air Waste Manage. Assoc.*, **1992**, *42*, 174–178.

[5] Russell, A.; Milford, J.; Bergin, M. S.; McBride, S.; McNair, L.; Yang, Y.; Stockwell, W. R.; Croes, B. *Science*, **1995**, *269*, 491–495.

[6] Khan, M.; Yang, Y.-J.; Russell, A. G. *Atmos. Environ.*, **1999**, *33*, 1085–1092.

[7] Yang, Y.-J.; Stockwell, W. R.; Milford, J. B. *Environ. Sci. Technol.*, **1995**, *29*, 1336–1345.

[8] Yang, Y.-J.; Stockwell, W. R.; Milford, J. B. *Environ. Sci. Technol.*, **1996**, *30*, 1392–1297.

[9] Bergin, M. S.; Russell, A. G.; Milford, J. B. *Environ. Sci. Technol.*, **1998**, *32*, 694–703.

[10] Carter, W. P. L. Documentation of the SAPRC99 chemical mechanism for VOC reactivity assessment. Final Report 92-329 and 95-308, Final Report to the California Air Resources Board, 2000.

[11] Carter, W. P. L. *Atmos. Environ.*, **1990**, *24A*, 481–518.

[12] Carter, W. P. L.; Luo, D.; Malkina, I. Environmental chamber studies for development of an updated photochemical mechanism for VOC reactivity assessment. Technical Report Contract 92-345, Final Report to the California Air Resources Board, 1997.

[13] DeMore, W. B.; Sander, S.; Golden, D. M.; Hampson, R. F.; Kurylo, M. J.; Howard, C. J.; Ravishankara, A. R.; Kolb, C. E.; Molina, M. J. Chemical kinetics and photochemical data for use in stratospheric modeling. Technical Report JPL Publication 97-4, Jet Propulsion Laboratory, Pasadena, CA, 1997. Evaluation No. 12. NASA Panel for Data Evaluation.

[14] Martien, P.; Harley, R.; Milford, J.; Hakami, A.; Russell, A. Development of reactivity scales via 3-D grid modeling of California ozone episodes. Final Report Con-

tract No. 98-309, California Air Resources Board, May 2002. Available online at http://www.arb.ca.gov/research/reactivity/harley.zip.

[15] Dunker, A. M. *J. Chem. Phys.*, **1984**, *81*, 2385–2393.

[16] Yang, Y.-J.; Wilkinson, J. G.; Russell, A. G. *Environ. Sci. Technol.*, **1997**, *31*, 2959–2868.

[17] McRae, G. J.; Goodin, W. R.; Seinfeld, J. H. *Journal of Computational Physics*, **1982**, *45*, 356–396.

[18] Goodin, W. R.; McRae, G. J.; Seinfeld, J. H. *J. Appl. Meteorol.*, **1979**, *18*, 761–771.

[19] Goodin, W. R.; McRae, G. J.; Seinfeld, J. H. *J. Appl. Meteorol.*, **1980**, *19*, 98–108.

[20] McNair, L. A.; Harley, R. A.; Russell, A. G. *Atmos. Environ.*, **1996**, *30*, 4291–4301.

[21] Main, H. H.; Lurmann, F. W.; Roberts, P. T. Pollutant concentrations along the western boundary of the south coast air basin. Part I: a review of existing data. Technical report, Sonoma Technology Inc., Santa Rosa, CA. Report to the South Coast Air Quality Management District., October 1990.

[22] Allen, P. D. Modeling Emissions Data System (MEDS) data files for southern California in summer 1987., February 1999. Personal communication, Planning and Technical Support Division, California Air Resources Board, Sacramento, CA, February 19, 1999.

[23] Harley, R. A.; Sawyer, R. F.; Milford, J. B. *Environ. Sci. Technol.*, **1997**, *31*, 2829–2839.

[24] Iman, R. L.; Shortencarier, M. J. A FORTRAN77 program and user's guide for the generation of Latin hypercube and random samples for use with computer models. Technical

Report SAND83-2365, U.S. Department of Energy, Sandia National Laboratory, Albuquerque, NM, 1984.

[25] Bergin, M. S.; Noblet, G. S.; Petrini, K.; Dhieux, J. R.; Milford, J. B.; Harley, R. A. *Environ. Sci. Technol.*, **1999**, *33*, 1116–1126.

[26] Wang, L.; Milford, J. B.; Carter, W. P. L. *Atmos. Environ.*, **2000**, *34*, 4349–4360.

[27] Carter, W. P. L. VOC reactivity data as of November 13, 2000. ftp.cert.ucr.edu/pub/carter/SAPRC99/r99tab.xls, 2000. Accessed August 2, 2001.

[28] Seinfeld, J. H.; Pandis, S. N. *Atmospheric Chemistry and Physics - From Air Pollution to Climate Change.*, page 312. Wiley, 1998.

[29] Yang, Y.-J.; Milford, J. B. *Environ. Sci. Technol.*, **1996**, *30*, 196–203.

Table 1: Chemical species represented explicitly.

Category	Code	Species Name	MW ($g\ mol^{-1}$)	MIR*	MOIR*
Alkane	CH4	methane	16.0	0.01	0.01
	C2H6	ethane	30.1	0.31	0.20
	N-C4	n-butane	58.1	1.33	0.83
	N-C5	n-pentane	72.1	1.54	0.95
	IPNT	isopentane	72.1	1.68	1.02
	MCPT	methyl cyclopentane	84.2	2.42	1.33
	224P	2,2,4-trimethylpentane	114.2	1.44	0.81
Alkene	ETHE	ethene	28.1	9.08	3.70
	PRPE	propene	42.1	11.58	4.43
	2MBT	2-methyl-2-butene	70.1	14.45	4.65
	BUTD	1,3-butadiene	54.0	13.58	4.83
	ISOP	isoprene	68.1	10.69	3.95
	APIN	α-pinene	136.2	4.29	1.56
	OLE1	lumped terminal olefins	70.1	7.79	3.11
Aromatic	C6H6	benzene	78.1	0.81	0.34
	TOLU	toluene	92.1	3.97	1.17
	XYLM	m-xylene	106.2	10.61	3.19
	XYLP	p-xylene	106.2	4.25	1.36
	124B	1,2,4-trimethylbenzene	120.2	7.18	2.32
Carbonyl	ACET	acetone	58.1	0.43	0.17
	MEK	methyl ethyl ketone	72.1	1.49	0.66
	HCHO	formaldehyde	30.0	8.97	2.56
	CCHO	acetaldehyde	44.1	6.84	2.56
	RCHO	propionaldehyde	58.1	7.89	2.97
	BALD	benzaldehyde	106.1	-0.61	-1.64
Other	C2H2	acetylene	26.0	1.25	0.49
	ETOH	ethanol	46.1	1.69	0.93
	IPOH	isopropanol	60.1	0.71	0.39
	MTBE	methyl tert-butyl ether	88.1	0.78	0.47
	BACT	n-butyl acetate	116.2	0.89	0.54
	CO	carbon monoxide	28.0	0.06	0.04

*MIR and MOIR values shown are from Carter [27].

Table 2: Inputs and parameters treated as random variables in the Monte Carlo with Latin hypercube sampling calculations

Parameter	COV	Notes	Parameter	COV	Notes
NO2 + $h\nu$	0.18	1	ARO2+HO	0.27	1
O3 + NO	0.1	1	PRPE+HO	0.14	1
O3 + $h\nu$	0.27	1	N-C4+HO	0.18	1
O1D2+H2O	0.18	1	224P+HO	0.18	1
O1D2+M	0.18	1	XYLM+HO	0.2	1,5,8
HO+NO2	0.27	1,6	ETOH+HO	0.18	1
HO+CO	0.27	1	DCB2,XYLM	0.3	2,5
HO2+NO	0.18	1	DCB3,XYLM	0.3	2,5
CCO-O2+NO2	0.16	1,7	MGLY,XYLM	0.3	2,5
PAN	0.4	1	EMCO	0.25	3
CCO-O2+NO	0.34	1	EMNX	0.06	3
PAN2	0.66	1	EMHC	0.06	3
RCO-O2+NO	0.75	1	EONX	0.15	3
HCHO+$h\nu$	0.34	1,9	EOHC	0.29	3
MEK+$h\nu$	0.42	1	DPO3	0.29	4
CRES+NO3	0.75	1	DPN2	0.29	4

1 Rate parameter of the indicated reaction treated as uncertain.

2 Dicarbonyl yield of the indicated product (DCB2, DCB3, or MGLY) from the reaction XYLM + HO treated as uncertain.

3 Uncertainty factors for emissions rates. EMCO is an uncertainty factor for general motor vehicle emissions, applied to CO, NO_x and NMOC (non-methane organic compounds). EMHC and EMNX are separate uncertainty factors for NMOC and NO_x emissions from motor vehicles, respectively. EOHC and EONX are uncertainty factors applied to other anthropogenic sources of NMOC and NO_x.

4 Deposition affinity for O_3 or NO_2 treated as random variable from a uniform distribution.

5 Uncertainty estimates for dicarbonyl yields (DCB2, DCB3, and MGLY) adapted from Wang et al. [26].

6 Correlated with DCB2, XYLM (ρ = 0.5); DCB3, XYLM (ρ = 0.5); and MGLY, XYLM (ρ = 0.5) based on Wang et al. [26].

7 Correlated with CCO-O2 + NO (ρ = 0.7).

8 Correlated with DCB2, XYLM (ρ = -0.6); DCB3, XYLM (ρ = -0.6); and MGLY, XYLM (ρ = -0.5) based on Wang et al. [26].

9 Applied to both HCHO + $h\nu \rightarrow 2HO_2$ + CO and HCHO + $h\nu \rightarrow H_2$ + CO.

Table 3: Uncertainty Contributions (UC, in %) of parameters contributing the most uncertainty in Absolute Incremental Reactivity (AIR; mean and COV) for the base mixture*.

Anaheim AIR = 0.11 (0.18) R^2 = 0.92		**Azusa** AIR = 0.13 (0.20) R^2 = 0.85		**Claremont** AIR = 0.13 (0.29) R^2 = 0.78		**Rubidoux** AIR = 0.10 (0.39) R^2 = 0.95	
Parameter	UC	Parameter	UC	Parameter	UC	Parameter	UC
NO2 + hv	22.8	**HCHO + hv**	20.1	**HO + NO2**	16.8	**EONX**	33.7
HCHO + hv	18.5	**CCO-O2 + NO**	12.7	DPN2	10.3	EOHC	18.2
DPO_3	10.6	**NO2 + hv**	10.9	**EONX**	9.8	DPN2	16.6
CCO-O2 + NO	8.5	**PAN**	6.6	EMHC	5.5	O_3 + hv	16.4
O_3 + hv	7.2	EONX	4.4	**NO2 + hv**	5.5	O1D2 + H2O	5.5
PAN	3.8	HO + NO2	3.9	EMCO	4.8	**O1D2 + M**	5.1
HO + NO2	3.6	**RCO-O2 + NO**	3.4	EOHC	4.1	HCHO + hv	3.5
HO2 + NO	3.4	**O_3 + hv**	3.1	**PAN**	3.8	EMHC	3.4

*Parameters in bold text have a positive regression coefficient; parameters in normal text have a negative regression coefficient.

Table 4: Uncertainty Contributions (UC, in %) of parameters contributing the most uncertainty in Relative Incremental Reactivity (RIR)*,**.

Anaheim		Azusa		Claremont		Rubidoux	
Parameter	UC	Parameter	UC	Parameter	UC	Parameter	UC
CO RIR = 0.04-0.07 (COV = 0.29-0.49)							
HO + CO	86.5	**HO + CO**	73.8	**HO + CO**	38.9	**HO + CO**	27.5
HO + NO2	6.2	HO + NO2	12.8	HO + NO2	33.2	**O_3 + hv**	15.5
O_3 + hv	4.5	DCB2,XYLM	3.5	**O_3 + hv**	6.6	**O1D2 + H2O**	11.1
HCHO + hv	3.6	EONX	2.6	**DPN2**	4.6	HO + NO2	6.8
ethanol (ETOH) RIR = 0.29-0.73 (COV = 0.22-0.34)							
ETOH + HO	26.5	**ETOH + HO**	49.6	**ETOH + HO**	28.7	**ETOH + HO**	18.8
CCO-O2 + NO	11.9	**CCO-O2 + NO**	15.2	**CCO-O2 + NO**	19.7	**PAN**	17.1
PAN	3.7	**PAN**	5.9	**PAN**	10.6	**CCO-O2 + NO**	16.0
RCO-O2 + NO	3.5	RCO-O2 + NO	3.3	RCO-O2 + NO	5.8	RCO-O2 + NO	11.3
HCHO RIR = 5.18-11.54 (COV= 0.14-0.35)							
HCHO + hv	27.5	**HO + NO2**	26.8	**HO + NO2**	44.2	O_3 + hv	29.2
O_3 + hv	20.5	**HCHO + hv**	20.9	O_3 + hv	11.3	**EONX**	11.0
EMCO	11.0	NO2 + hv	12.8	NO2 + hv	9.4	**O1D2 + M**	8.9
O1D2 + M	8.8	MEK + hv	7.5	**EONX**	5.8	O1D2 + H2O	7.5
MEK RIR = 0.30-0.80 (COV = 0.32-0.37)							
MEK + hv	71.6	**MEK + hv**	75.0	**MEK + hv**	53.9	**MEK + hv**	44.8
HO + NO2	7.0	HCHO + hv	13.4	**HO + NO2**	22.0	**HO + NO2**	14.8
HCHO + hv	5.5	**HO + NO2**	10.9	HCHO + hv	12.7	O_3 + hv	6.6
O_3 + hv	3.4	**EONX**	2.1	DPN2	3.2	HCHO + hv	6.3
n-butane (N-C4) RIR = 0.31-0.53 (COV = 0.18-0.26)							
N-C4 + HO	48.7	**N-C4 + HO**	59.2	HO + NO2	42.3	**O_3 + hv**	25.6
O_3 + hv	11.3	HO + NO2	14.7	**N-C4 + HO**	25.3	**N-C4 + HO**	20.7
EMCO	6.0	**O_3 + hv**	4.6	**EOHC**	11.0	HO + NO2	13.3
HCHO + hv	5.8	**NO2 + hv**	2.5	**O_3 + hv**	9.6	**O1D2 + H2O**	11.1
propene (PRPE) RIR = 7.17-8.45 (COV = 0.08-0.09)							
PRPE + HO	27.0	**PRPE + HO**	38.1	EMCO	18.1	MEK + hv	18.6
224P + HO	19.2	MEK + hv	18.0	224P + HO	15.6	**PRPE + HO**	15.2
N-C4 + HO	15.3	224P + HO	11.8	MEK + hv	14.1	224P + HO	12.4
RCO-O2 + NO	8.0	N-C4 + HO	4.3	**PRPE + HO**	13.5	PAN2	8.0
2,2,4-trimethylpentane (224P) RIR = 0.60-0.91 (COV = 0.18-0.29)							
224P + HO	47.5	**224P + HO**	39.6	HO + NO2	39.2	**224P + HO**	15.4
HO + NO2	14.5	HO + NO2	31.0	**224P + HO**	19.2	**O_3 + hv**	12.4
O_3 + hv	9.6	**HCHO + hv**	13.9	**HCHO + hv**	13.1	HO + NO2	7.4
RCO-O2 + NO	4.4	EONX	3.8	**EOHC**	9.2	**O1D2 + H2O**	6.8
m-xylene (XYLM) RIR = 6.82-8.30 (COV = 0.14-0.34)							
HCHO + hv	27.6	HCHO + hv	39.1	HCHO + hv	27.3	O_3 + hv	18.2
DCB2,XYLM	17.7	**DCB2,XYLM**	21.3	**HO + NO2**	24.0	HCHO + hv	15.1
XYLM + HO	13.8	**XYLM + HO**	19.8	**DCB2,XYLM**	5.8	**HO + NO2**	12.5
HO + NO2	8.9	MEK + hv	5.8	O_3 + hv	4.8	**DCB2,XYLM**	9.1

*Parameters in bold text have a positive correlation coefficient; parameters in normal text have a negative correlation coefficient.

**R^2 values for the uncertainty analysis range from 0.81 - 0.98.

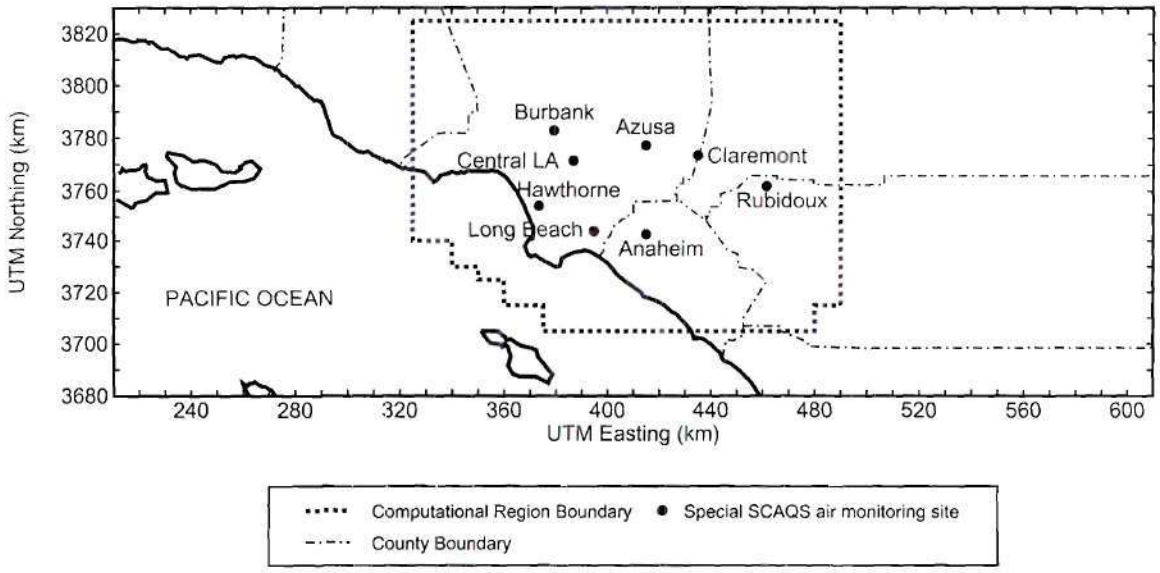

Figure 1: Modeling domain with selected measurement sites and the boundary of the computational region.

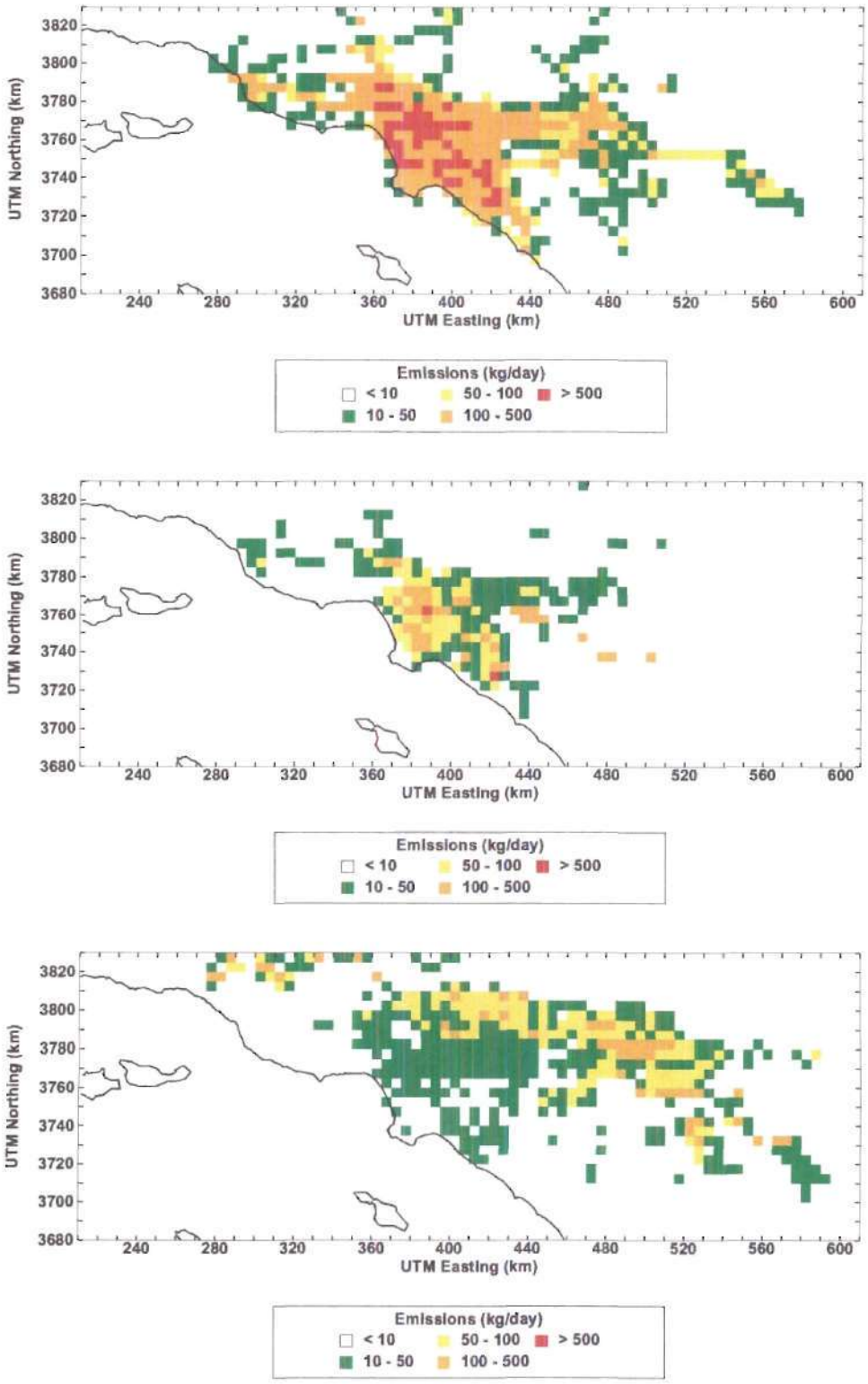

Figure 2: Estimated emissions in kg/day per grid cell on 25 June 1987 for (a) propene, (b) isopropanol, and (c) isoprene.

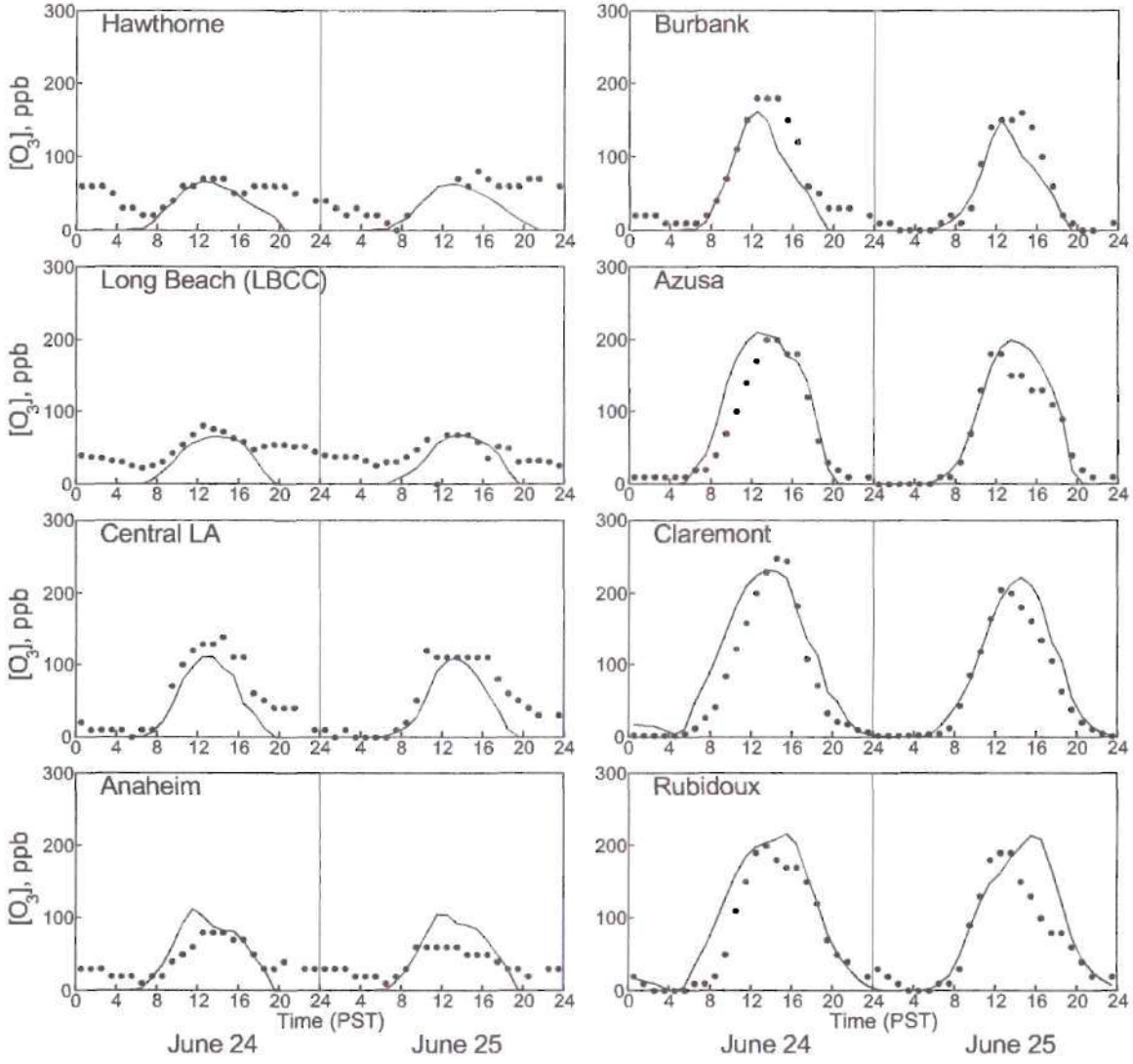

Figure 3: Ozone time series plots comparing observed (circles) and predicted (line) surface-level ozone at coastal sites Hawthorne and Long Beach, at central sites Central LA and Anaheim, and at inland sites Burbank, Azusa, Claremont, and Rubidoux.

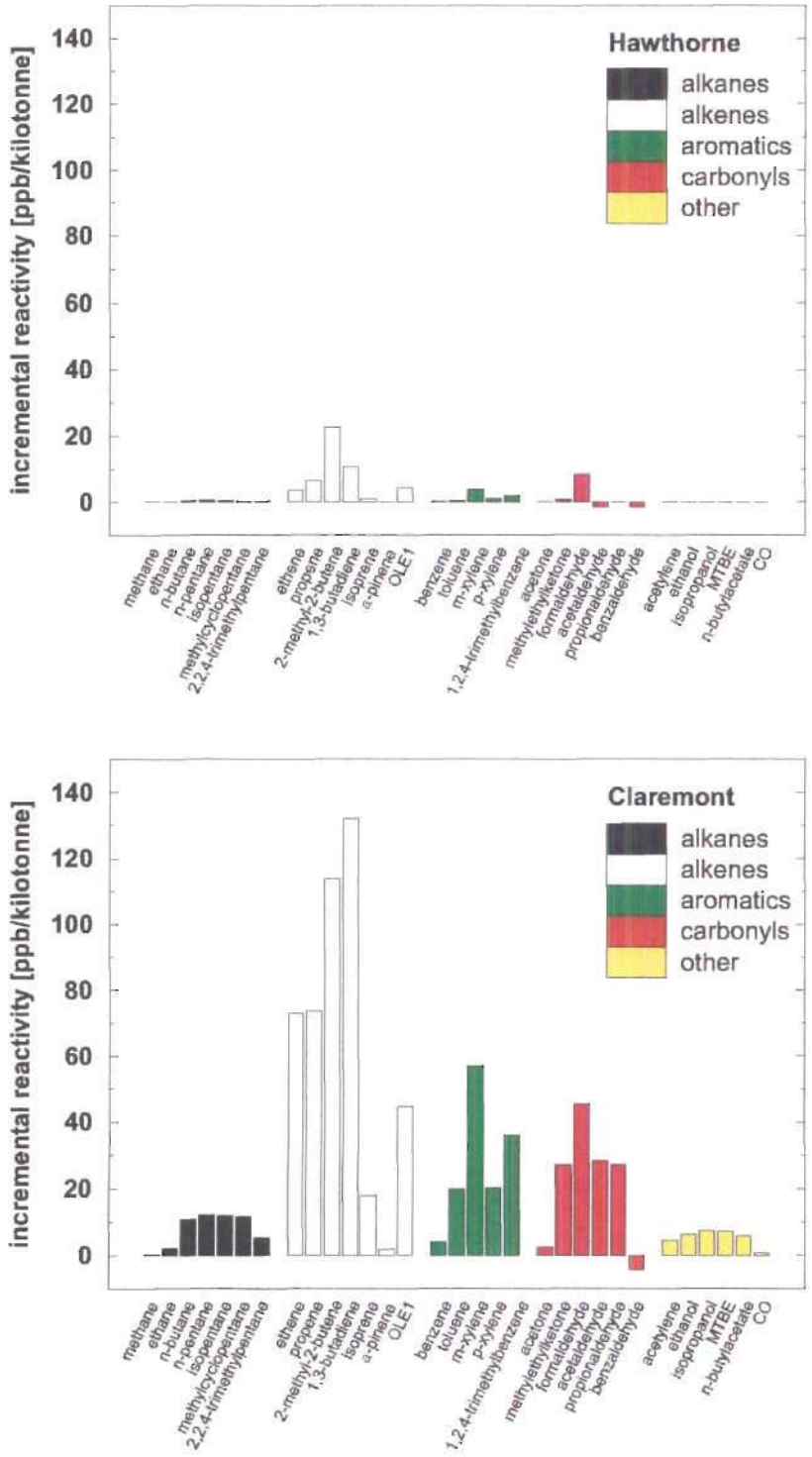

Figure 4: Absolute incremental reactivities calculated at the time of maximum observed ozone on 25 June 1987 at (a) coastal site Hawthorne and (b) inland site Claremont.

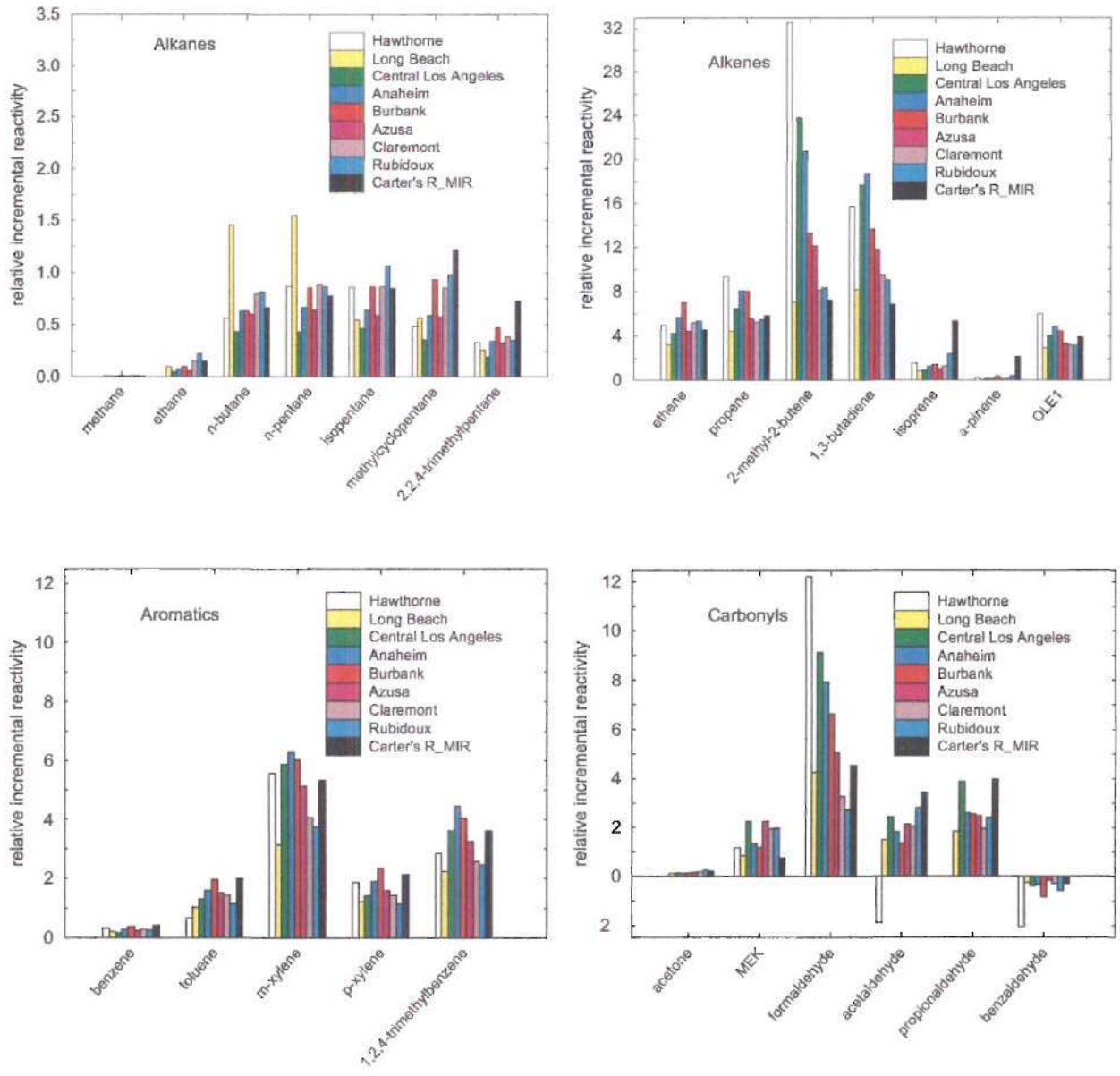

Figure 5: Relative incremental reactivities calculated at the time of maximum ozone on 25 June 1987 at all sites for (a) alkanes, (b) alkenes, (c) aromatics, and (d) carbonyls. R_MIR values from Carter [27] are included for comparison.

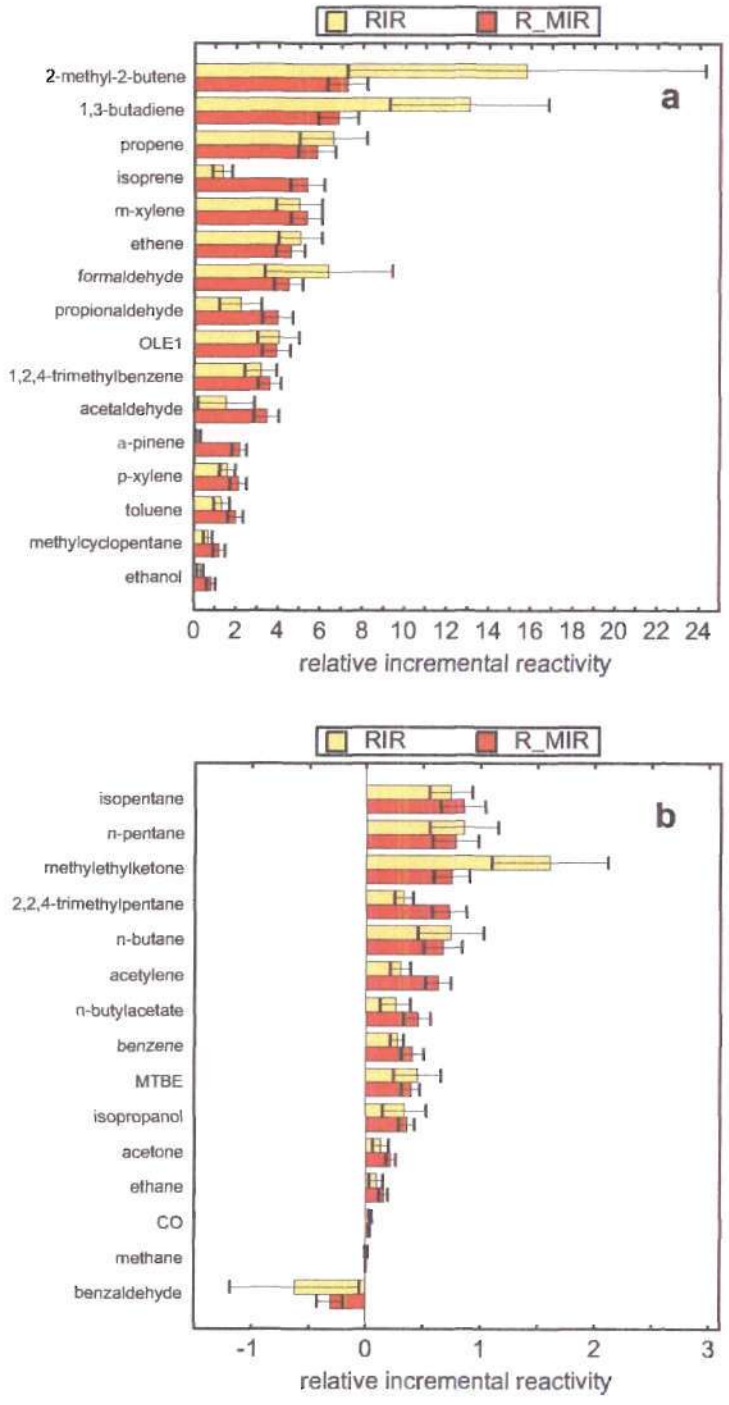

Figure 6: Sorted average Relative Incremental Reactivity (RIR; $\pm 1\sigma$, 8 sites) calculated at the time of maximum ozone on 25 June 1987 and R_MIR ($\pm 1\sigma$, 39 cities) for (a) the most reactive species and (b) the least reactive species. The sort order is based on R_MIR.

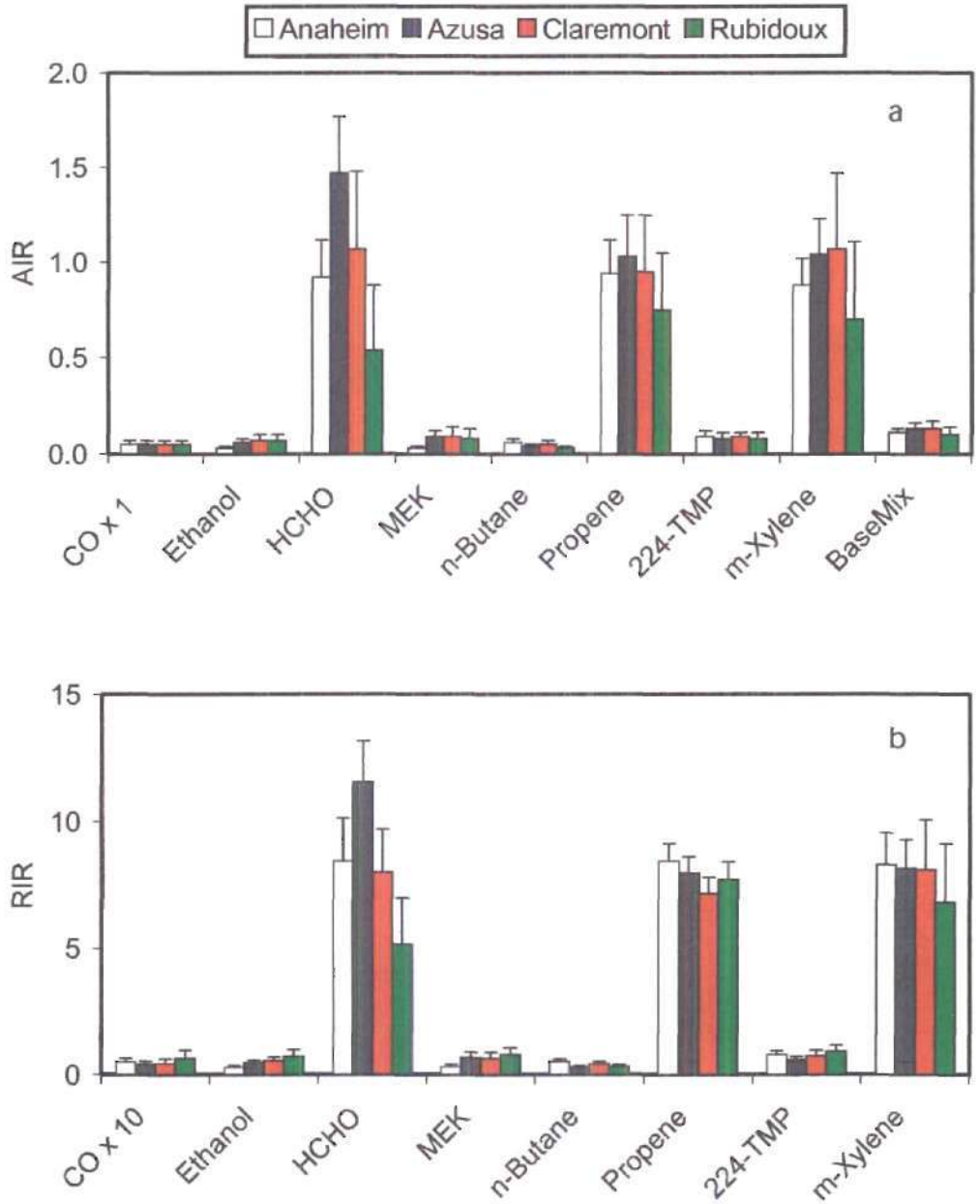

Figure 7: (a) Absolute incremental reactivities and associated uncertainties for selected compounds and the base mixture, and (b) relative incremental reactivities and associated uncertainties for selected compounds. Note 224-TMP is 2,2,4-trimethylpentane.

Figure Captions

Figure 1 Modeling domain with selected measurement sites and the boundary of the computational region.

Figure 2 Estimated emissions in kg/day per grid cell on 25 June 1987 for (a) propene, (b) isopropanol, and (c) isoprene.

Figure 3 Ozone time series plots comparing observed (circles) and predicted (line) surface-level ozone at coastal sites Hawthorne and Long Beach, at central sites Central LA and Anaheim, and at inland sites Burbank, Azusa, Claremont, and Rubidoux.

Figure 4 Absolute incremental reactivities calculated at the time of maximum observed ozone on 25 June 1987 at (a) coastal site Hawthorne and (b) inland site Claremont.

Figure 5 Relative incremental reactivities calculated at the time of maximum ozone on 25 June 1987 at all sites for (a) alkanes, (b) alkenes, (c) aromatics, and (d) carbonyls. R_MIR values from Carter [27] are included for comparison.

Figure 6 Sorted average Relative Incremental Reactivity (RIR; $\pm 1\sigma$, 8 sites) calculated at the time of maximum ozone on 25 June 1987 and R_MIR ($\pm 1\sigma$, 39 cities) for (a) the most reactive species and (b) the least reactive species. The sort order is based on R_MIR.

Figure 7 (a) Absolute incremental reactivities and associated uncertainties for selected compounds and the base mixture, and (b) relative incremental reactivities and associated uncertainties for selected compounds. Note 224-TMP is 2,2,4-trimethylpentane.

Table Captions

Table 1 Chemical species represented explicitly.

Table 2 Inputs and parameters treated as random variables in the Monte Carlo with Latin hypercube sampling calculations

Table 3 Uncertainty Contributions (UC, in %) of parameters contributing the most uncertainty in Absolute Incremental Reactivity (AIR; mean and COV) for the base mixture*.

Table 4 Uncertainty Contributions (UC, in %) of parameters contributing the most uncertainty in Relative Incremental Reactivity (RIR)*,**.